DYNAMIC SIMULATION OF A ROLLER RIG

A. Anyakwo[1], C. Pislaru, A. Ball and F. Gu
[1] University of Huddersfield, Queensgate, HD1 3DH, UK

ABSTRACT

The dynamic behaviour of railway vehicles is greatly influenced by the interaction of the wheelsets on the railway track. This behaviour can be replicated in laboratory conditions using a scaled roller rig.
This paper presents the results of the modeling and simulation of a one-fifth scale roller rig. The simulation results obtained have been compared with a real railway vehicle (bogie) on the track. It has been observed that the scale roller rig has a much lower critical velocity than real railway vehicle due to the similarity and dimensional scaling laws that are taken into consideration in the roller rig design. The scale roller rig critical speed was observed to be 10.2 m/s while the Full Scale railway vehicle model was found to be 52 m/s. It can be concluded that the critical speed of the scaled roller rig model is one-fifth of the full scale critical speed.

Keywords modelling simulation scale roller rig critical speed

1 INTRODUCTION

Railway vehicles have become one of the most important transportation systems in our society today. For controlled testing of the dynamic stability of a railway vehicle in laboratory conditions, roller rigs suffice for investigations of the dynamic behaviour of railway vehicles so as to improve the suspension designs and stability. Several studies on the application of roller rigs can be found in a number of literatures. (Hur et al. 2009) studied the influence of wheel profile wear on scale bogie stability using critical speed tests. The numerical models for full scale roller rig and 1/5th scale rig contained the wheel-rail contact models (including the wear parameters – flange thickness, flange height, wear factor and flange contact angle) and were implemented in MATLAB. Four dynamic tests with various critical speeds were performed and the wear parameters were determined from the wheel profiles measured with mini-prof. The critical speeds for the full scale test rig were inversely proportional to equivalent conicity of the wheel profile (which increased with the wheel flange wear).
(Jaschinski et al. 1999) discussed the application of roller rigs to railway vehicle dynamic applications. Different roller rig designs were presented and discussed along with their advantages and disadvantages. It was of the opinion that roller rigs are vital for testing and experimental purposes and for validation real railway vehicle dynamic simulations. However the scaling problems of roller rigs which occur as a result of dimensional and similarity laws are the major set-backs for the application of roller rigs since these affect the dynamic response of the rig and results differ from that a railway vehicle running on a track. (Allen and Iwnicki 2001) used a roller rig to investigate the dynamic behaviour of railway vehicles. He computed the critical velocity of the roller rig and compared the same results with simulations of a full scale roller rig. Errors in simulation results where as a result of scaling and correlation reduction between scale roller rigs and full-scale vehicles.
This paper presents the non-linear differential equations of motion for a full scale model and a 1/5 scale roller rig. These equations have been solved using ode23 solver from MATLAB software. Using the Heuristic non-linear creep force model, the differential equations of the roller rig governing the dynamic performance of the 4 DOF system are derived. The gyroscopic motion of the wheel sets on the rollers have been neglected here since they do not have much effect on the dynamic response of the bogie system

2 NON-LINEAR DIFFERENTIAL EQUATIONS OF MOTION

The differential equations of motion used to simulate the dynamic model of a typical bogie are expressed in Equations (1 – 6). The bogie frame and the wheelset are allowed to move in the yaw and lateral directions. The creep forces developed at the contact points were determined using Heuristic non-linear creep force model (S. Iwnicki 2003).

.

$$m\frac{d^2y_1}{dt^2} = F_{yr1} + F_{yl1} + N_{ry1} - N_{ly1} + F_{susp1} \quad (1)$$

$$m\frac{d^2y_2}{dt^2} = F_{yr2} + F_{yl2} + N_{ry2} - N_{ly2} + F_{susp2} \quad (2)$$

$$I_z\frac{d^2\psi_1}{dt^2} = -l_o(F_{xl1} - F_{xr1}) + (R_{rx1} + R_{rr1}) * \left(F_{yr1} + N_{ry1}\right) - (R_{lx1} + R_{ll1})(F_{yl1} + N_{ly1}) \quad (3)$$

$$I_z\frac{d^2\psi_2}{dt^2} = -l_o(F_{xl2} - F_{xr2}) + (R_{rx2} + R_{rr2}) * \left(F_{yr2} + N_{ry2}\right) - (R_{lx2} + R_{ll2})(F_{yl2} + N_{ly2}) \quad (4)$$

$$m_b\frac{d^2y_3}{dt^2} = F_{susp1} + F_{susp2} \quad (5)$$

$$I_b\frac{d^2\psi_3}{dt^2} = b(F_{susp1} + F_{susp2}) - (M_{susp1} + M_{susp2}) \quad (6)$$

Where:

m = mass of the wheelset (kg)
m_b = mass of Bogie frame (kg)
I_z = Yaw moment of inertia of wheelset (kgm^2)
I_b = Yaw moment of inertia of the Bogie frame (kgm^2)
y_1 = Lateral displacement of wheelset 1 (m)
y_1 = Lateral displacement of wheelset 2 (m)
ψ_1 = Yaw displacement of wheelset 1 (radians)
ψ_2 = Yaw displacement of wheelset 2 (radians)
F_{xr1} = Longitudinal creep force of right wheel 1 (N)
F_{xl1} = Longitudinal creep force of left wheel 1 (N)
F_{xr2} = Longitudinal creep force of right wheel 2 (N)
F_{xl2} = Longitudinal creep force of left wheel 2 (N)
F_{yr1} = Lateral contact force of right wheel 1 (N)
F_{yl1} = Lateral contact force of left wheel 1 (N)
I_b = Yaw moment of inertia of the Bogie frame (kgm^2)
y_1 = Lateral displacement of wheelset 1 (m)
y_1 = Lateral displacement of wheelset 2 (m)
ψ_1 = Yaw displacement of wheelset 1 (radians)
ψ_2 = Yaw displacement of wheelset 2 (radians)
M_{susp2} = Suspension moment wheelset 2 (N)
l_o = Half wheelset gauge (mm)
R_{rx1} = Longitudinal contact position right wheel 1 (m)
R_{rx2} = Longitudinal contact position right wheel 2 (m)
R_{lx1} = Longitudinal contact position left wheel 1 (m)
Rl_{x2} = Longitudinal contact position left wheel 2 (m)
I_b = Yaw moment inertia of the Bogie frame (kgm^2)
y_1 = Lateral displacement of wheelset 1 (m)
y_1 = Lateral displacement of wheelset 2 (m)
ψ_1 = Yaw displacement of wheelset 1 (radians)
ψ_2 = Yaw displacement of wheelset 2 (radians)
F_{xr1} = Longitudinal creep force of right wheel 1 (N)
F_{xl1} = Longitudinal creep force of left wheel 1 (N)
F_{xr2} = Longitudinal creep force of right wheel 2 (N)
F_{xl2} = Longitudinal creep force of left wheel 2 (N)
F_{yr1} = Lateral contact force of right wheel 1 (N)
F_{yl1} = Lateral contact force of left wheel 1 (N)
F_{yr2} = Lateral contact force of right wheel 2 (N)
F_{yl2} = Lateral contact force of left wheel 2 (N)
M_{zr1} = Spin creep moment of right wheel 1 (N)
M_{zl1} = Spin creep moment of left wheel 1 (N)
M_{zl2} = Spin creep moment of left wheel 2 (N)
F_{susp1} = Suspension force wheelset 1 (N)
F_{susp2} = Suspension force wheelset 2 (N)
M_{susp1} = Suspension moment wheelset 1 (N)

N_{ry1} = Lateral normal contact force right wheel 1 (m)
N_{ry2} = Lateral normal contact force right wheel 2 (m)
N_{ly1} = Lateral normal contact force left wheel 1 (m)
Nl_{y2} = Lateral normal contact force left wheel 2 (m)
b = wheelset base

3 WHEEL-RAIL GEOMETRY ANALYSIS

The wheel-rail geometry was realized assuming new P8 wheel and BS 110A rail profiles. The contact point locations were determined using two dimensional wheel-rail geometry analyses where the lateral displacement and the roll angle are used as inputs. The locations of the contact points on the wheel and the rail where determined by solving the geometrical constraint equations arising from the profile geometry.

The contact point positions on the left and right rail for a positive lateral displacement is shown in Fig. 3(c) and 3(d). The rolling radius difference function, the contact angle and the equivalent conicity results are derived from the wheel-rail contact geometry.

The rolling radius function is proportional to the rate of change of the lateral displacement. At 5.5mm, the wheelset flange makes the first contact with the rail gauge. At 7 mm there is sharp contact jump and the rolling radius difference increases sharply in this region. After 7 mm the increase in the rolling radius difference increases as well and wheelset flange climb occurs. The contact angle function is derived from the derivative of the rail lateral contact co-ordinate function with respect to the lateral displacement. At 7 mm the contact angle is very large and it reaches about 2.3 radians (69 degrees). It can also be observed that there is a large contact jump from 5.5 mm to 7 mm in the contact angle function. The equivalent conicity function is an approximation that accounts for the average slope of the rolling radius difference function over a finite range of the lateral displacement of the wheelset on the rail. Given that the rolling radius difference function is expressed as follows:

$$R(y) = 2\lambda y \tag{7}$$

Where R(y) is the rolling radius difference function, λ is the effective conicity and y is the lateral displacement, the equivalent conicity calculated via the trapezoidal rule can be expressed as follows:

$$\lambda_e = \frac{1}{4\Delta y^2}\int_{-\Delta y}^{\Delta y} R(y)dy \tag{8}$$

Where the lateral displacement range is from -Δy to + Δy (Thomsen & True 2010).
The contact angle function difference function and the rolling radius function is shown in Fig. 3(a) and Fig. 3(b) respectively.

4 WHEEL-RAIL CONTACT FORCES

The wheel-rail contact forces are developed as a result of creepages emanating from the contact patch. These creepages arise as a result of traction, braking, acceleration due to the relative motion of the wheel on the rail. The creep forces developed as a result are the lateral, longitudinal and spin moment creep forces. They can be defined as follows (S. Iwnicki 2003):

$$F_{yr,l} = -Ga_{r,,}b_{r,,}C_{22}v_{yr,l} - Ga_{r,l}b_{r,l}\sqrt{a_{r,l}b_{r,l}}C_{23}v_{spinr,l} \tag{9}$$

$$F_{xr,l} = -Ga_{r,,}b_{r,,}C_{11}v_{xr,l} \tag{10}$$

$$M_{zr,l} = Ga_{r,,}b_{r,,}\sqrt{a_{r,l}b_{r,l}}C_{23}v_{yr,l} - GabC_{33}\left(a_{r,l}b_{r,l}\right)^2 v_{spinr,l} \tag{11}$$

Where $F_{yr,l}$ *is the* lateral creep force for the right and left wheel, $F_{xr,l}$ is the longitudinal creep force for the right and left wheel while $M_{zr,l}$ is the spin creep moment of the right and left wheel. G is the rigid modulus of rigidity, $a_{r,l}$ and $b_{r,l}$ are the semi-axis of the elliptical wheel-rail contact patch. $v_{yr,l}$, $v_{xr,l}$ and $v_{spinr,l}$ are the lateral, longitudinal and spin creepages for the right and left wheel rail contact respectively.
For typical wheel-roller contact geometry the creepages are calculated slightly differently due to the de-crowing effect of the wheelset on the rollers. The de-crowning effect leads to a large yaw angle developed at the by the wheelset on the roller. Hence the angular velocity of the rollers and the radius of the rollers are taken into account when calculating the creepages. This adds extra value to the longitudinal, lateral and spin creep moment creepages derived for a wheel-rail contact (Allen & S. D. Iwnicki 2001). It is important to note that Equations (9 – 11) are the wheel-rail contact creep forces developed by Kalker. These forces are linear in the wheel tread region as long as the creepages developed in the contact patch is very small. For large creepages arising as a result of flange contact with the results Kalker's linear creep forces is no longer valid. Hence non-linear creep force models are applied to limit the creep forces. In this paper the non-linear Heuristic model has been applied to limit the creep forces.

5 SUSPENSIONS FORCES

The forces developed at the suspension are a function of the lateral displacement of the wheelsets, lateral displacement of the bogie frame, yaw angle of the wheelsets, yaw angle of the bogie, lateral velocity of the wheelsets and bogie and yaw velocity of the wheelsets and bogie. The suspension force on wheelset 1 is:

$$F_{susp1} = -2K_{py}(-y_1 + y_b - b\,\psi_b) - 2\dot{C_{py}}(-\dot{y}_1 + \dot{y}_b - b\,\dot{\psi}_b) \tag{12}$$

$$F_{susp2} = -2K_{py}(-y_2 + y_b + b\,\psi_b) - 2\dot{C_{py}}(-\dot{y}_2 + \dot{y}_b + b\,\dot{\psi}_b) \tag{13}$$

where K_{py}/C_{py} is the lateral stiffness/lateral damping of the spring. y_1 and y_2 are the lateral displacement of the front and rear wheelsets respectively. y_b is the lateral displacement of the bogie, and ψb and $\dot{\psi}_b$, are the yaw angle bogie and yaw velocity of the bogie respectively. $\dot{y}_1$, $\dot{y}_2$ and $\dot{y}_b$ are the lateral velocity of the front, rear and bogie respectively.
The suspension moment forces can be expressed as:

$$M_{susp1} = 2b^2K_{px}(-\psi_1 + \psi_b) + 2b^2C_{px}(-\dot{\psi}_1 + \dot{\psi}_b) \quad (14)$$

$$M_{susp2} = 2b^2K_{px}(-\psi_2 + \psi_b) + 2b^2C_{px}(-\dot{\psi}_2 + \dot{\psi}_b) \quad (15)$$

Where Kpx is the longitudinal spring stiffness and Cpx is the longitudinal damper coefficient.

6 SCALE ROLLER RIG MODEL

The 1/5 scaled bogie model is designed and implemented using the same equations defined in Equations (1 -6) but with adjustments in the creepages developed at the contact patch due to the variation of velocity on the roller head and a minute longitudinal velocity introduced roller head when it is yawed. Also the roller circumferential velocity is considered as an additional term to the lateral and spin creepages developed in a real railway wheel-rail contact patch during modelling. The scale roller rig is shown in Fig.1 and Fig 2.

There are usually scaling imperfections especially in scaling the modulus of rigidity and gravitational acceleration. Using MMU scale roller rig as a case study, the scaling factor for time is equal to one while the rig dimensions are also scaled down to one-fifth of the full scale vehicle model.

The table showing the Full Scale model and the 1/5 scale roller rig model is shown below. Note that α = 5 for the scaled roller rig model.

Table 1: Full Scale Model and 1/5 Scale roller rig model parameters

Parameters	Full Scale Model	Scale	1/5 Scale roller rig
Wheelset mass m (kg)	1587.5	m/α^3	12.7
Bogie mass m_b (kg)	2612.5	m_b/α^3	20.9
Wheelset Yaw moment of inertia I_z (kgm^2)	1000	I_z/α^5	0.32
Bogie Yaw moment of inertia I_b (kgm^2)	3937.5	I_b/α^5	1.26
Lateral stiffness of primary suspension K_{py} (N/m)	4.5×10^6	K_{py}/α^3	36×10^3
Longitudinal primary suspension stiffness K_{px} (N/m)	12.5×10^6	K_{px}/α^3	100×10^3
Lateral damping of primary suspension C_{py} (Ns/m)	3.33×10^5	C_{py}/α^3	2.67×10^3
Longitudinal damping of suspension C_{px} (Ns/m)	1.51×10^6	C_{px}/α^3	12.05×10^3
Wheelbase b (m)	1.25	b/α	0.25
Wheel radius R_o (m)	0.5	R_o/α	0.1
Roller radius R_r (m)	0.5	R_r/α	0.18
Gauge l_o (m)	1.435	l_o/α	0.287

7 SIMULATION RESULTS FOR THE SCALE ROLLER RIG AND FULL SCALE ROLLER RIG

Simulations where carried out by reducing Equations (1 – 6) to first order differential equations and then solving the equations completely using Ode solvers in MATLAB precisely Ode23s solver. This solver solves stiff non-linear differential equations using Rosenbrock's method for solution of ordinary differential equations. The twelve state variable used for simulation are the lateral displacement of wheelset one and two, yaw angle of wheelset one and two, lateral velocity of wheelset one and two, yaw velocity of wheelset one and two, lateral displacement of bogie, yaw displacement of bogie, lateral velocity of bogie and yaw velocity of bogie. The differential equations of the full scale model and the scale roller rig model were solved completely with initial conditions given to the state variables.

Given the initial values of the lateral displacements, at low forward speeds, the wheelsets return to a central position hence the system is stable. As the forward speed increases, the wheelset lateral behaviour on the track becomes unstable and hunting results. The forward speed at which hunting occurs is referred to as the critical velocity of the vehicle. Using the primary suspension parameters of the scaled roller rig and the full scale model, the forward speed was gradually increased until flange contact with the rail gauge occurred. It is imperative to note that the flange clearance is given as 5.5 mm (0.0055m) as can be observed from the rolling radius difference function. The critical velocity at which hunting occurs for the full scale model was determined as 52 m/s while the critical velocity for the scale roller rig was found to be 10.2 m/s. The results of the simulation given an initial lateral

displacement of 0.0055 m for the front wheelset and -0.0055 m for the rear wheelset are shown in Fig. 4 and Fig. 5.
It can be observed from the simulations that the critical velocity of the scale roller rig model and the full scale model is related to the scale used. The critical velocity of the scale roller rig is approximately one-fifth of the critical velocity of the full scale roller rig.

8 CONCLUSIONS

This paper presents the calculation of the critical speeds for a typical full scale railway vehicle model and a 1/5 scale roller rig model. The non-linear mathematical equations for these models have been solved using MATLAB ordinary differential equation solver ode23s. The creepages and the creep forces developed at the wheel-rail contact have been determined. The critical speed for the full scale model was 52 m/s while 1/5 scale roller rig model had the critical velocity (maximum value before hunting occurs) of 10.2 m/s. The additional errors in the creepages as a result of the roller velocities can be improved by controlling the movement of the rollers under the wheelset.

REFERENCES

HUR, H-M., PARK. J-H., YOU. W-H., and PARK T-W., (2009). A study on the critical speed of worn wheel profile using a scale model. *Journal of Mechanical Science and Technology*, 23 (10), pp.2790-2800.

JASCHINSKI A., CHOLLET H., IWNICKI S. D., WICKENS A.H., and VON WURZEN J., (1999).The Application of Roller Rigs to Railway Vehicle Dynamics. *Vehicle System Dynamics*, 31(5-6), pp. 345-392.

ALLEN, P.D. and IWNICKI, S.D., (2001).The critical speed of a railway vehicle on a roller rig. *Proceedings of the Institution of Mechanical Engineers, Part F: Journal of Rail and Rapid Transit*, 215(2), pp.55 -64.

IWNICKI S. D,(2003). Simulation of wheel–rail contact forces. *Fatigue & Fracture of Engineering Materials & Structures*, 26(10), pp. 887-900.

THOMSEN, P.G. and TRUE, H.,(2010). *Non-smooth Problems in Vehicle Systems Dynamics: Proceedings of the Euromech 500 Colloquium*, Springer.

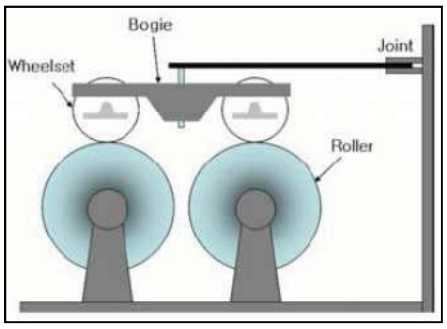

Fig.1 Scale Roller rig Model (Hur et al. 2009)

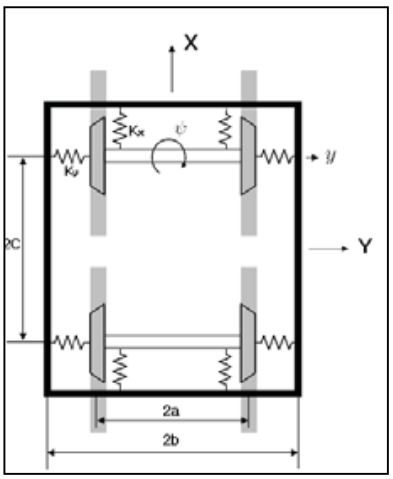

Fig. 2 Plan view of the Scale Roller bogie model (Hur et al. 2009)

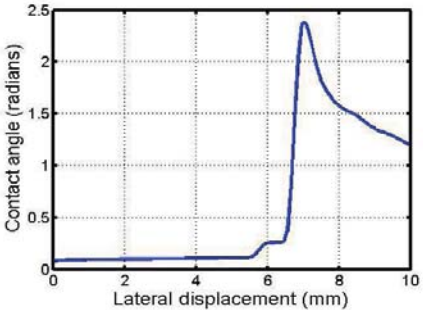

(a) Contact angle function

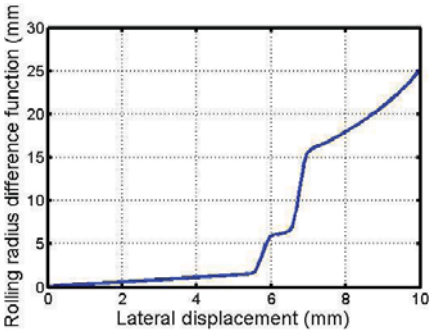

(b) Rolling radius difference function

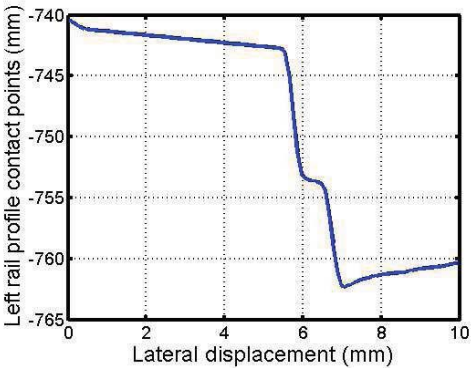

(c) Left rail contact position

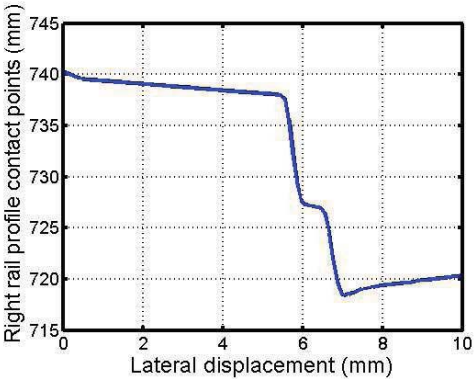

(d) Right rail contact position

Fig. 3 Wheel rail contact geometry results

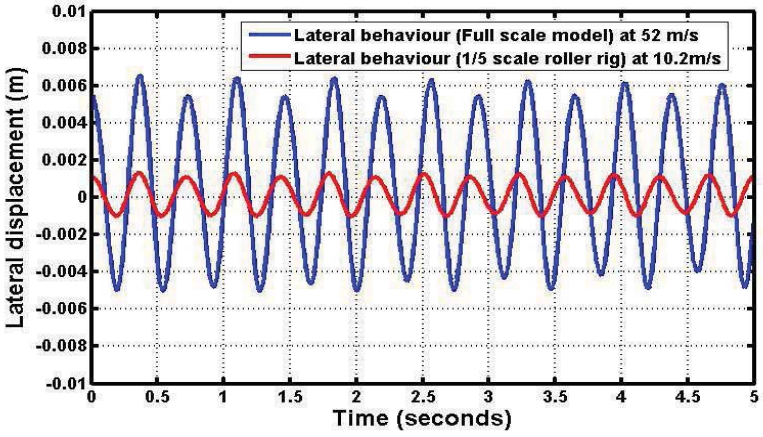

Fig. 4: Simulated lateral displacement of front wheelsets for the two rigs

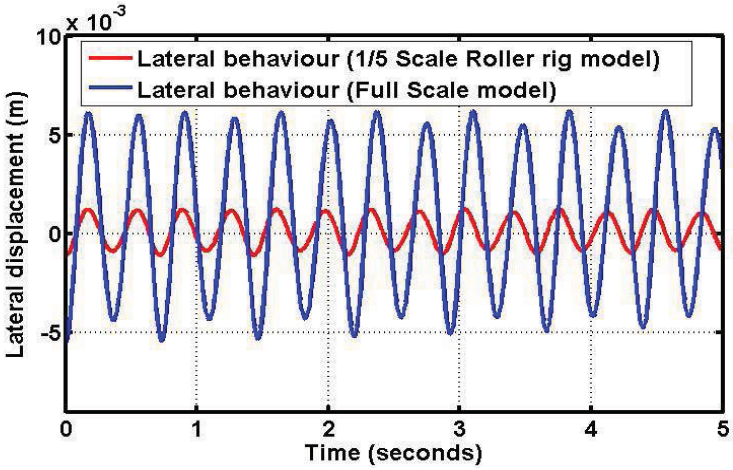

Fig. 5: Simulated lateral displacement of rear wheelsets for the two rigs